DC-DC/AC Boost Converter With Battery Storage-A Burp Char Technique

1. R.Rajitha,PG Student,2.C.Balachandra Reddy,Professor&HOD
Department of EEE,CBTVIT,Hyderabad

Abstract-This paper presents a new extendable single-stage multi-input dc–dc/ac boost converter. The proposed structure comprises of two bidirectional ports in the converter's central part to interface output load and battery storage, and several unidirectional input ports to get powers from different input dc sources. In fact, the proposed topology consists of two sets of parallel dc–dc boost converters, which are actively controlled to produce two independent output voltage components. Choosing two pure dc or two dc-biased sinusoidal values as the converter reference voltages, situations of the converter operating in two dc–dc and dc–ac modes are provided, respectively. The proposed converter utilizes minimum number of power switches and is able to step up the low-level input dc voltages into a high-level output dc or ac voltage without needing any output filter. The converter control system includes several current regulator loops for input dc sources and two voltage regulator loops for generating the desired output voltage components, resulting in autonomously charging/discharging the battery to balance the power flow. Due to the converter inherent multi-input multioutput control system, the small signal model of the converter is extracted and then the pole-placement control strategy via integral state feedback is applied for achieving the converter control laws. The validity and effectiveness of the proposed converter and its control performance are verified by simulation and experimental results.

Index Terms—Hybrid systems, multi input converter, single stage converter, small-signal modeling, state feedback.

I. INTRODUCTION

Energy sources like wind turbines and photovoltaic (PV) systems are intermittent and unpredictable; therefore, they are not highly reliable. In order to address this issue, renewable resources are either combined with each other or fuel cells (FCs) and energy storage systems (ESSs). Nowadays, the concept of multiple-input converters (MICs) has been proposed to accommodate several renewable energy resources. These converters provide simple circuit topologies, centralized control, high reliability, low manufacturing cost, and size. The systematic approaches of generating and synthesizing MICs have been introduced in [1]–[4]. In general, all various MICs are responsible to accept dc voltage sources at their input ports, while from the output point of view they can be broken into two categories: dc–dc MICs and dc–ac MICs.

For the first category, in [5]–[7], three multi-input converters have been proposed based on the structure of the dc boost converter. The three-input dc–dc boost converter proposed by the authors in [7] benefits from simple unified structure and minimum numbers of power switches. A family of multiport dc–dc converters based on the combination of dc-link voltages by magnetic coupling of half-bridge boost converters has been presented in [8]. In [9] and [10] two hybrid dc–dc systems were introduced and their control strategies have been planned based on decoupling method to separately compensate the cross coupled control loops. In [11], a systematic approach is proposed for the derivation of non isolated three-port converter topologies.

Although dc–ac MICs gain several advantages, all of them utilize at least two conversion stages and need an output filter to support ac loads. Accordingly, for all MICs, multiple power conversion stages may result in increasing the count of devices, system power losses, size, weight, and cost of hybrid systems.

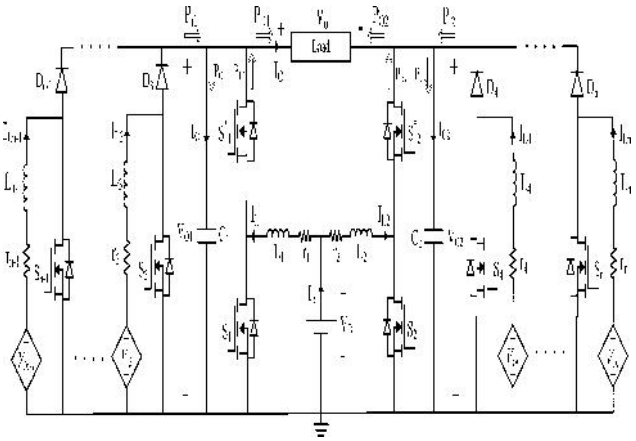

Fig. 1. Proposed converter structure

A three-port dc–dc converter integrating PV and battery powers for high step-up applications is proposed in [12]. For the second category, i.e., dc–ac MICs, in [13], an isolated dc–ac bidirectional multi-input converter has been controlled by the input-output feedback linearization method. An isolated three-port full-bridge topology has been proposed in [14] for hybrid FC/Battery systems, which aims at feeding a small autonomous load. A line-interactive FC power supply has been introduced in [15], which can operate in both stand-alone and grid-connected modes. A grid connected multi-input inverter has been proposed in [16] to form a hybrid PV/wind power system.

In this regard, single-stage topologies, which integrate performance of each stage of multistage power converters, are becoming more attractive. Although they may cause control complexity, they offer higher efficiency and reliability, and lower cost and size. In [17], a single-stage single-input z-source inverter with coupled inductor, which is able to step-up low-level input dc voltages into a high-level output ac voltage, has been proposed. In [18], two dc sources are embedded in the x-shape impedance network of the z-source inverter. This circuit lacks enough degrees of freedom for the control system and does not provide acceptable current ripple for the input sources. Conventional single-stage boost inverter [19] has been

utilized by the authors as a series grid-connected single-stage PV inverter in [20], which also plays the role of grid voltage compensator for an ac load. Unfortunately, all single-stage inverters are not multi-input and therefore not suitable for hybrid systems. As discussed previously, it can be said that for multisource systems, better performances can be accessed providing that a single stage multiinput converter is utilized. Such a converter becomes more attractive if it can operate in both dc–dc and dc–ac modes, without any changes in the converter structure.

In this paper, a new extendable single-stage multi-input boost converter is proposed which can operate in both dc–dc and dc– ac modes. The proposed converter integrates two bidirectional ports for battery storage and output load and several unidirectional ports for different input dc sources. The proposed converter is able to directly step up the low-level input dc voltages into a high-level output dc/ac voltage and does not need any output filter, while it only uses the minimum number of power switches. The load voltage is differentially obtained from the converter two output voltage components. For dc–dc mode operation, these voltages are regulated at two different dc values, while in dc–ac mode they are controlled to be two 180◦ out-ofphase dc-biased sinusoidal voltages. Owing to the multi-input structure of the converter, the integral state feedback strategy of multi-input multioutput (MIMO) control systems is applied to the converter small signal model to achieve its control laws. As a result, several input current regulator loops for the input dc sources and two output voltage control loops are designed for the proposed converter. Finally, the effectiveness of the proposed converter and its control performance are studied and verified by simulation and experimental results.

In comparison with other multi-input double-stage dc–ac converters, the proposed converter applies only one power conversion stage and also is able to operate in both dc–dc and dc–ac modes without using any output filter. To be more precise, it utilizes less number of power switches and passive elements.

Moreover, compared to a system that utilizes the same number of active and/or passive elements, the proposed system has superiority over minimizing voltage ratings and sizes of the elements.

II. LITERATURE SURVEY

DC-DC BOOST CONVERTER

The boost is a popular non-isolated power stage topology, sometimes called a step-up power stage. Power supply designers choose the boost power stage because the required output is always higher than the input voltage. The input current for a boost power stage is continuous, or non-pulsating, because the output diode conducts only during a portion of the switching cycle. The output capacitor supplies the entire load current for the rest of the switching cycle.

Figure 1 shows a simplified schematic of the boost power stage. Inductor L and capacitor C make up the effective output filter. The capacitor equivalent series resistance (ESR), RC, and the inductor dc resistance, RL, are included in the analysis. Resistor R represents the load seen by the power supply output.

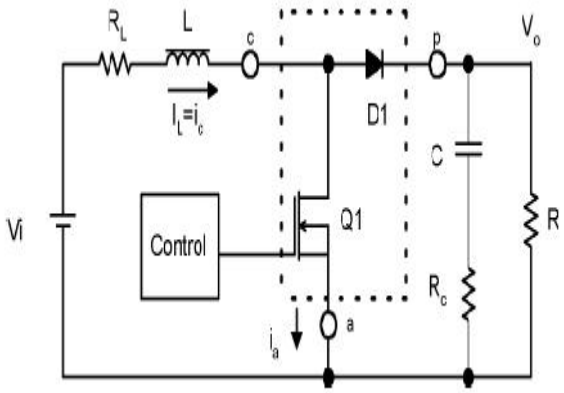

Figure 1. Boost Power Stage Schematic

A power stage can operate in continuous or discontinuous inductor current mode. In continuous inductor current mode, current flows continuously in the inductor during the entire switching cycle in steady-state operation. In discontinuous inductor current mode, inductor current is zero for a portion of the switching cycle. It starts at zero, reaches peak value, and return to zero during each switching cycle. It is desirable for a power stage to stay in only one mode over its expected operating conditions because the power stage frequency response changes significantly between the two modes of operation.

2.1Boost Steady-State Continuous Conduction Mode (CCM):

In continuous conduction mode, the boost power stage assumes two states per switching cycle. In the on state, Q1 is on and D1 is off. In the off state, Q1 is off and D1 is on. A simple linear circuit can represent each of the two states where the switches in the circuit are replaced by their equivalent circuit during each state. Figure 2 shows the linear circuit diagram for each of the two states.

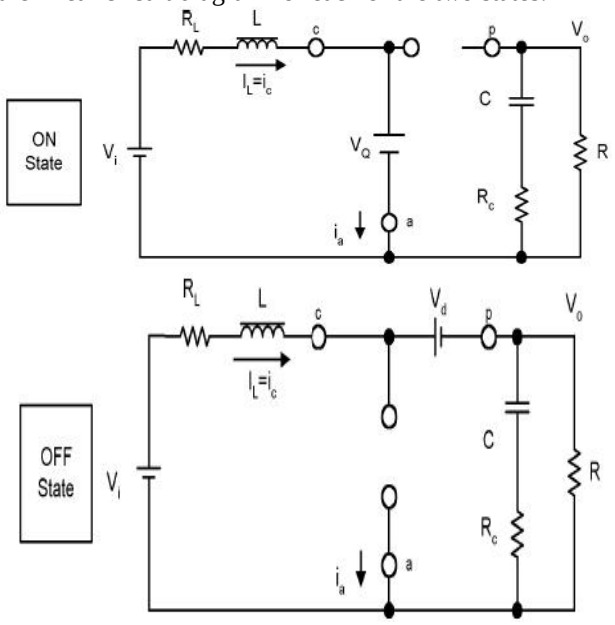

Figure 2 Boost Power Stage States

The duration of the on state is D×Ts=TON, where D is the duty cycle set by the control circuit, expressed as a ratio of the switch on time to the time of

one complete switching cycle, Ts . The duration of the off state is TOFF.

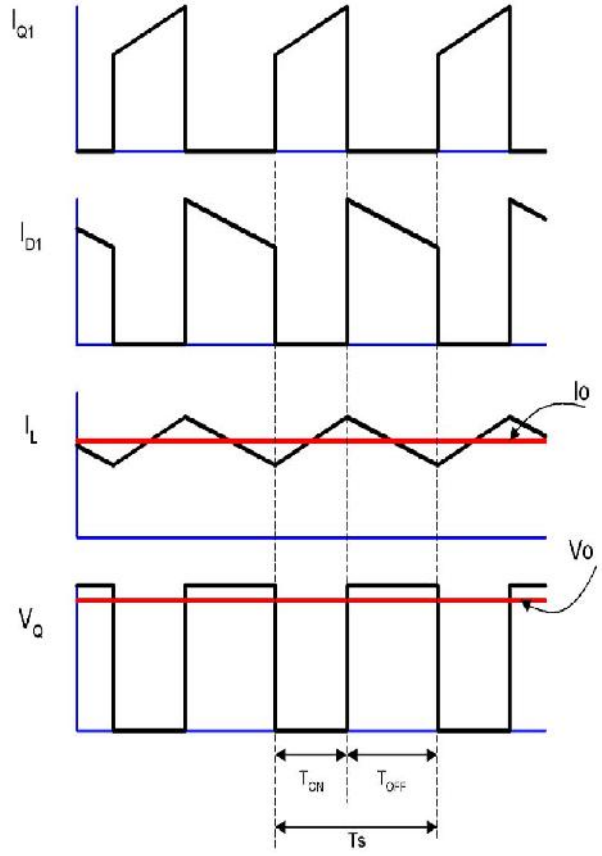

Figure 3 CCM Boost Power Stage Waveforms

Refer to Figures 1 and 2. The inductor-current increase can be calculated by using a version of the familiar relationship:

$$V_L = L \times \frac{di_L}{dt} \Rightarrow \Delta I_L = \frac{V_L}{L} \Delta T$$

The inductor current increase during the on state is given by:

$$\Delta I_L(+) = \frac{V_i - (V_Q + I_L \times R_L)}{L} \times T_{ON}$$

The quantity ΔIL(+) is the inductor ripple current. During this period, all of the output load current is supplied by output capacitor C.

The inductor current decrease during the off state is given by:

$$\Delta I_L(-) = \frac{(V_O + V_d + I_L \times R_L) - V_i}{L} \times T_{OFF}$$

The quantity ΔIL(-) is also the inductor ripple current.

In steady-state conditions, the current increase, ΔIL(+), during the on time and the current decrease, ΔIL(-), during the off time are equal. Therefore, these two equations can be equated and solved for VO to obtain the continuous conduction mode (CCM) boost voltage conversion relationship:

$$V_O = (V_i - I_L \times R_L) \times (1 + \frac{T_{ON}}{T_{OFF}}) - V_d - V_Q \times (\frac{T_{ON}}{T_{OFF}})$$

And,

$$D = \frac{T_{ON}}{T_{ON} + T_{OFF}} = \frac{T_{ON}}{T_S} \qquad (1 - D) = \frac{T_{OFF}}{T_S}$$

The steady-state equation for VO is:

$$V_O = \frac{V_i - I_L \times R_L}{1 - D} - V_d - V_Q \times \frac{D}{1 - D}$$

**Notice that in simplifying the above, TON+TOFF is assumed to be equal to Ts. This is true only for CCM mode.*

The above voltage conversation relationship for VO illustrates that VO can be adjusted by adjusting the duty cycle, D, and is always greater than the input because D is a number between 0 and 1. A common simplification is to assume VQ, Vd, and RL are small enough to ignore. The above equation simplifies considerably to:

$$V_O = \frac{V_i}{1 - D} \qquad I_O = (1 - D) \times I_i$$

A simplified, qualitative way to visualize the circuit operation is to consider the inductor as an energy storage element. When Q1 is on, energy is added to the inductor. When Q1 is off, the inductor and the input voltage source deliver energy to the output capacitor and load. The output voltage is controlled by setting the on time of Q1. For example, by increasing the on time of Q1, the amount of energy delivered to the inductor is increased. More energy is then delivered to the output during the off time of Q1 resulting in an increase in the output voltage.

To relate the inductor current to the output current, refer to Figure 2 and 3. Note that the inductor delivers current to the output only during the off state of the power stage. This current averaged over a complete switching cycle is equal to the output current because the average current in the output capacitor must be equal to zero. The relationship between the average inductor current and the output current for the CCM mode is given by:

$$I_{L(Avg)} \times \frac{T_{OFF}}{T_S} = I_{L(Avg)} \times (1 - D) = I_O \Rightarrow I_{L(Avg)} = \left(\frac{I_O}{1 - D}\right)$$

2.2Boost Steady-State Discontinuous Conduction Mode (DCM):

Figure 4 shows the inductor current condition where the power stage is at the boundary between continuous and discontinuous mode. This is where the inductor current just falls to zero and the next switching cycle begins immediately after the current reaches zero. From the charge and discharge of output capacitor, the output current is given by:

$$I_O \times (T_{ON} + T_{OFF}) = \frac{I_{PK}}{2} \times T_{OFF} \Rightarrow I_{PK} = \frac{2 \times I_O}{1 - D}$$

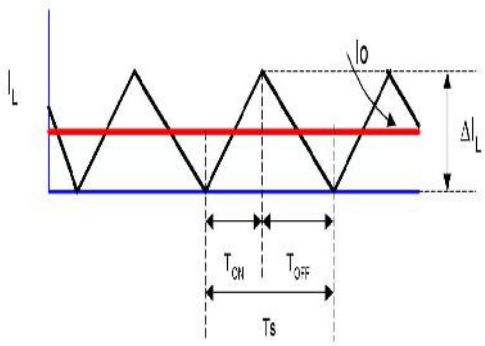

Figure 4. Boundary Between Continuous and Discontinuous Mode

Further reduction in output load current puts the power stage into discontinuous current conduction mode (DCM). The discontinuous mode power stage input-to output relationship is quite different from the continuous mode.

III. PROPOSED METHOD AND RESULTS

PROPOSED CONVERTER AND OPERATION MODES

The structure of the proposed extendable single-stage multi input dc–dc/ac boost converter is illustrated in Fig. 1. As indicated in the figure, in the converter central part, two bidirectional ports are provided to connect the output load and battery storage. The output load is connected between two dc-link voltages *VO*1 and *VO*2 , which are unipolar and independently obtained from the voltages across two common output capacitors of several parallel dc boost converters. The middle boost converters are current bidirectional and connected to the dc-link of the common battery, while the other ones (i.e., $i = 3, \ldots, n$) are current unidirectional and fed from separate input dc source (i.e., *Vi*3 , . . . , *V*in). The first aim of using the battery storage is to supply or absorb the power difference between the total generated dc power by the input dc sources and the load power.

In this hybrid system, all kind of rechargeable batteries and also ultra capacitors are applicable as ESS. For the proposed system, the single power switch of each unidirectional boost converter is controlled to regulate the dc power of its corresponding input source, while in the converter central part both upper and lower power switches of the bidirectional boost converters are complementary switched to produce their corresponding output reference voltages. Thus, *n* different duty ratios (*d*1 , . . . , and *dn*) are introduced to control the converter power switches *S*1, *S* 1, *S*2, *S* 2, *S*3 , . . . , and *Sn*, respectively.

These duty ratios are the converter controlling variables that facilitate current and voltage regulation goals of the proposed system. For the proposed system, the input dc sources *Vi*3 , . . . , *V*in should deliver *n*-2 ripple free dc currents, i.e., *IL*3 , . . . , *ILn*, respectively. Thus, the total generated dc powers at the both sides of the converter are expressed as follows:

$$P_{i_1} = \sum_{k=2}^{n/2} V_{i_{2k-1}} I_{L_{2k-1}}, \quad P_{i_2} = \sum_{k=2}^{n/2} V_{i_{2k}} I_{L_{2k}}.$$

(1)

The proposed converter can work in both dc–dc and dc–ac modes. Following sections will try to demonstrate operation principles of the proposed converter in these operation modes.

4.1 DC–DC Mode:

If two different dc values are chosen as the converter output reference voltages, then a pure dc voltage appears across the output load as follows:

$$Vo1 = V1, \; Vo2 = V2 \; , \; Vo = V1 - V2.$$

(2)

For an output resistive load the consumed power can be expressed by the following equations:

$$I_o = (V_1 - V_2)/R_L$$
$$P_o = V_o I_o = (V_1^2 - 2V_1V_2 + V_2^2)/R_L.$$

(3)

Now, we obtain the converter first- and second-side powers *Po*1 and *Po*2 delivered to the load as follows:

$$P_{o_1} = V_{o_1} I_o = (V_1^2 - V_1V_2)/R_L$$
$$P_{o_2} = -V_{o_2} I_o = -(V_1V_2 - V_2^2)/R_L.$$

(4)

As seen in (4), first side of the converter delivers the positive power amount *PO*1, while the negative power amount of *PO*2 is absorbed by the converter second side. These powers are constant values that only depend on the converter both side voltages. By neglecting converter power losses, the battery's both sides powers are obtained as follows:

$$P_{B_1} = P_{o_1} - P_{i_1} = \frac{(V_1^2 - V_1V_2)}{R_L} - \sum_{k=2}^{n/2} V_{i_{2k-1}} I_{L_{2k-1}}$$
$$P_{B_2} = P_{o_2} - P_{i_2} = -\frac{(V_1V_2 - V_2^2)}{R_L} - \sum_{k=2}^{n/2} V_{i_{2k}} I_{L_{2k}}.$$

(5)

The summation of *PB*1 and *PB*2 gives the battery total exchanged power as follows:

$$P_B = P_{B_1} + P_{B_2} = P_o - \sum_{k=3}^{n} V_{i_k} I_{L_k}.$$

(6)

As (6) shows, the battery source supplies or absorbs the power difference between the load power and the total generated input power. The battery current *IB* and its both side inductor currents *IL*1 and *IL*2 are determined as follows:

$$\begin{cases} I_{L_1} = \dfrac{P_{B_1}}{V_B} = \dfrac{P_{o_1} - P_{i_1}}{V_B} \\ I_{L_2} = \dfrac{P_{B_2}}{V_B} = \dfrac{P_{o_2} - P_{i_2}}{V_B} \end{cases}; \quad I_B = \frac{P_o}{V_B} - \sum_{k=3}^{n} \frac{V_{i_k} I_{L_k}}{V_B}$$

(7)

4.2 DC–AC Mode:

If the converter reference voltages are chosen as (8), then the proposed converter will operate in the dc–ac mode as

$$V_{o1}(t) = V_{dc} + \frac{V_m}{2}\text{Sin}\,\omega t$$

$$V_{o2}(t) = V_{dc} - \frac{V_m}{2}\text{Sin}\,\omega t$$

(8)

where their dc parts are the same as *V*dc and the modulation of each sinusoidal part is 180◦ out of phase with the other one. This concept results in generating a pure sinusoidal voltage across the load as follows:

$$Vo\,(t) = Vo1\,(t) - Vo2\,(t) = Vm\text{Sin}\,\omega t.$$

(9)

Instantaneous current and power of an output resistive load can be expressed by the following equations:

$$I_o(t) = I_m \text{Sin}\,\omega t, \quad I_m = V_m / R_L$$

$$P_o(t) = V_o(t) I_o(t) = \bar{P}_o + \tilde{P}_o = -\frac{V_m I_m}{2}\text{Cos}\,2\omega t + \left[\frac{V_m I_m}{2}\right].$$

(10)

In (10), the average quantity (*VmIm*)/2 corresponds to the load average power $\bar{}$ *Po* , while the alternative term at the angular frequency of *2ω* denotes the pulsation component of the load power. Now, the converter first- and second-sides instantaneous powers delivered to the load are obtained as follows:

$$P_{o1} = V_{o1}(t) I_o(t) = V_{dc} I_m \text{Sin}\,\omega t + \frac{V_m I_m}{2}\text{Sin}^2 \omega t$$

$$= V_{dc} I_m \text{Sin}\,\omega t - \frac{\bar{P}_o}{2}\text{Cos}\,2\omega t + \left[\frac{\bar{P}_o}{2}\right]$$

$$P_{o2} = -V_{o2}(t) I_o(t) = -V_{dc} I_m \text{Sin}\,\omega t - \frac{\bar{P}_o}{2}\text{Cos}\,2\omega t + \left[\frac{\bar{P}_o}{2}\right]$$

(11)

As (11) shows, the average powers delivered to the load at the both sides of the converter are the same and equal to the half of the load average power for all power operation conditions.

Also, the instantaneous powers associated with the converter capacitors *C*1 and *C*2 (*XC*1 = *1/C*1*ω* and *XC*2 = *1/C*2*ω*) are obtained as follows:

$$P_{C_1} = V_{o_1} I_{C_1} = \left(V_{dc} + \frac{V_m}{2}\text{Sin}\,\omega t\right)\frac{C_1 d}{dt}\left(V_{dc} + \frac{V_m}{2}\text{Sin}\,\omega t\right)$$

$$= \frac{V_{dc} V_m}{2X_{C_1}}\text{Cos}\,\omega t + \frac{V_m^2}{8X_{C_1}}\text{Sin}\,2\omega t$$

$$P_{C_2} = V_{o_2} I_{C_2} = -\frac{V_{dc} V_m}{2X_{C_2}}\text{Cos}\,\omega t + \frac{V_m^2}{8X_{C_2}}\text{Sin}\,2\omega t.$$

(12)

Neglecting the converter power losses and the stored energy in the converter inductors, the battery's both side powers are obtained as follows:

$$P_{B_1} = P_{o_1} + P_{C_1} - P_{i_1} = V_{dc} I_m \text{Sin}\,\omega t + \frac{V_{dc} V_m}{2X_{C_1}}\text{Cos}\,\omega t$$

$$- \frac{\bar{P}_o}{2}\text{Cos}\,2\omega + \frac{V_m^2}{8X_{C_1}}\text{Sin}\,2\omega t$$

$$+ \left[\frac{\bar{P}_o}{2} - \sum_{k=2}^{n/2} V_{i_{2k-1}} I_{L_{2k-1}}\right]$$

$$P_{B_2} = P_{o_2} + P_{C_2} - P_{i_2} = -V_{dc} I_m \text{Sin}\,\omega t - \frac{V_{dc} V_m}{2X_{C_2}}\text{Cos}\,\omega t$$

$$- \frac{\bar{P}_o}{2}\text{Cos}\,2\omega t + \frac{V_m^2}{8X_{C_2}}\text{Sin}\,2\omega t + \left[\frac{\bar{P}_o}{2} - \sum_{k=2}^{n/2} V_{i_{2k}} I_{L_{2k}}\right]$$

(13)

Summing *PB*1 and *PB*2 and assuming *XC*1 = *XC* 2 = *XC* gives the total instantaneous battery power as follows:

$$P_B = \bar{P}_B + \tilde{P}_B = -\bar{P}_o \text{Cos}\,2\omega t + \frac{V_m^2}{4X_C}\text{Sin}\,2\omega t$$

$$+ [\tilde{P}_o - P_{i_1} - P_{i_2}]$$

(14)

where $\bar{}$ *PB* represents the battery average power, which is equal to the system power difference between the total generated dc power and the average load power. Besides, the power component ˜ *PB* is the summation of the pulsation component of the load power and the total reactive power associated with the converter capacitors. Now, neglecting the saved energy in the converter inductors, the battery current and its both side inductors currents are obtained

$$I_{L_1} = \frac{P_{B_1}}{V_B} = \frac{V_{dc} I_m}{V_B}\text{Sin}\,\omega t + \frac{V_{dc} V_m}{2V_B X_C}\text{Cos}\,\omega t$$

$$- \frac{\bar{P}_o}{2V_B}\text{Cos}\,2\omega t + \frac{V_m^2}{8V_B X_C}\text{Sin}\,2\omega t + \left[\frac{\bar{P}_o - 2P_{i_1}}{2V_B}\right]$$

$$I_{L_2} = \frac{P_{B_2}}{V_B} = -\frac{V_{dc} I_m}{V_B}\text{Sin}\,\omega t - \frac{V_{dc} V_m}{2V_B X_C}\text{Cos}\,\omega t$$

$$- \frac{\bar{P}_o}{2V_B}\text{Cos}\,2\omega t + \frac{V_m^2}{8V_B X_C}\text{Sin}\,2\omega t + \left[\frac{\bar{P}_o - 2P_{i_2}}{2V_B}\right]$$

(15)

$$I_B = \frac{P_B}{V_B} = -\frac{\bar{P}_o}{V_B}\text{Cos}\,2\omega t + \frac{V_m^2}{4V_B X_C}\text{Sin}\,2\omega t$$

$$+ \left[\frac{\bar{P}_o - P_{i_1} - P_{i_2}}{V_B}\right]$$

(16)

As seen in (15), two currents *IL*1 and *IL*2 contain two similar alternative terms with the angular frequencies of *ω* and *2ω* and two different dc terms that depend on the total generated power by their corresponding input dc sources. Moreover, the battery current in (16) is a dc-biased sinusoidal waveform at the angular frequency of *2ω*, which guarantees supplying the expected dc and ac power components of the battery.

Simulink model

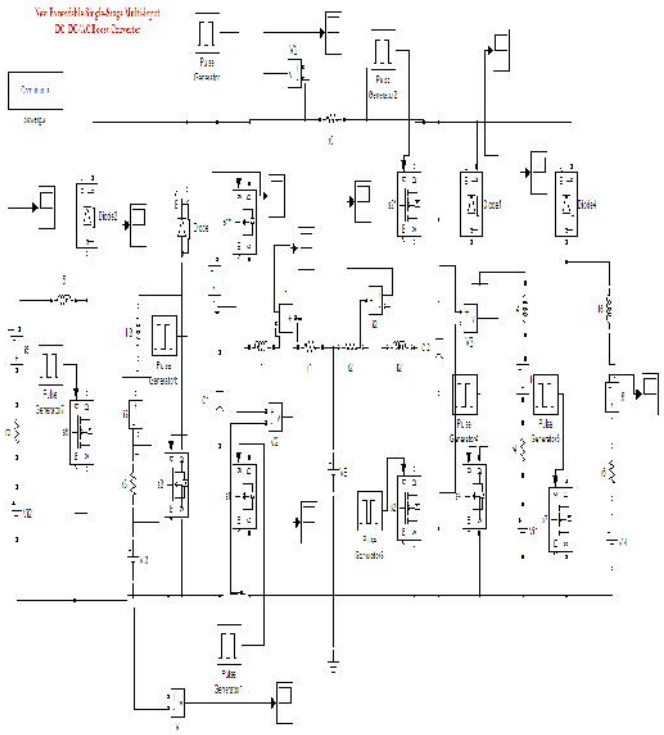

Fig: Simulation circuit

Results:

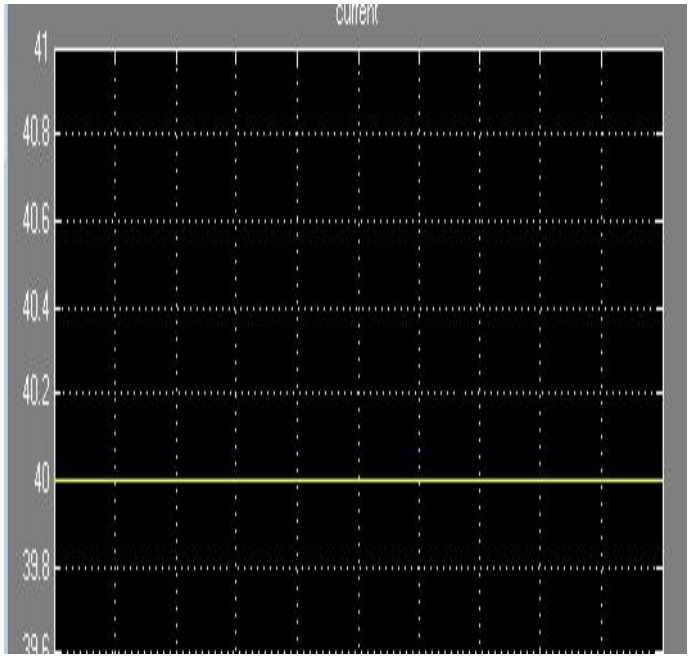

Fig:input current

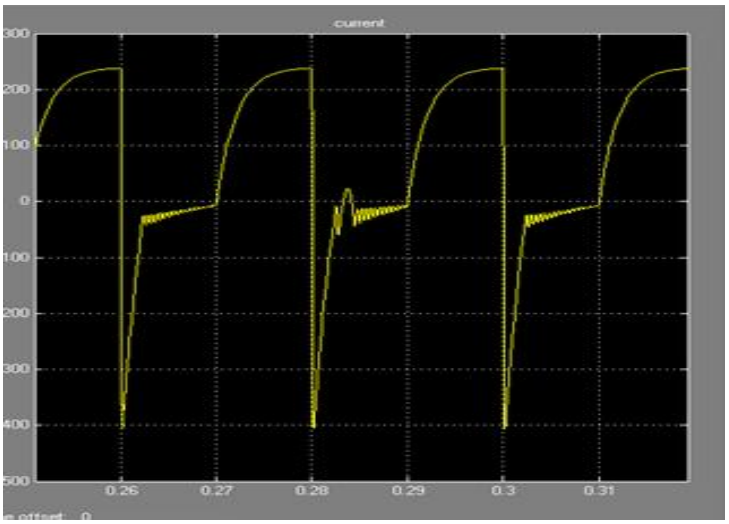

Fig:output current

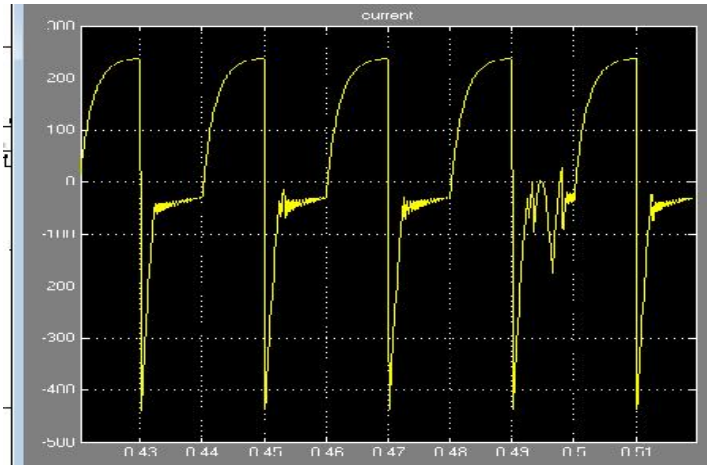

Fig:output current

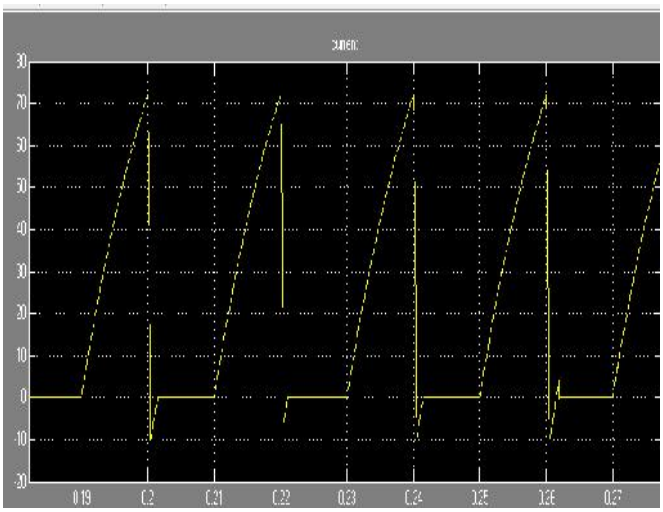

Fig: variation in currents

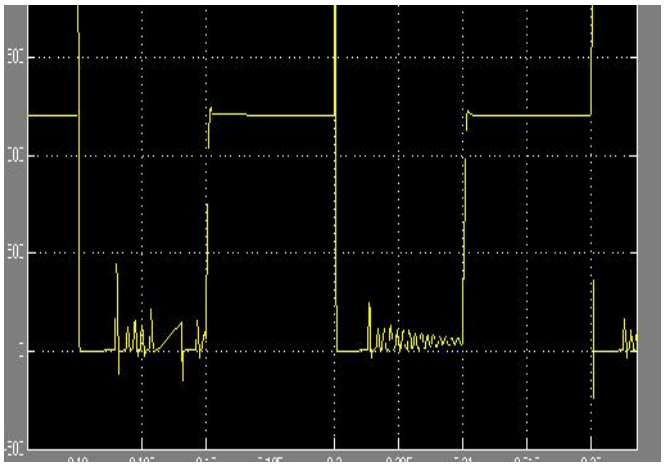

Fig:Input voltag

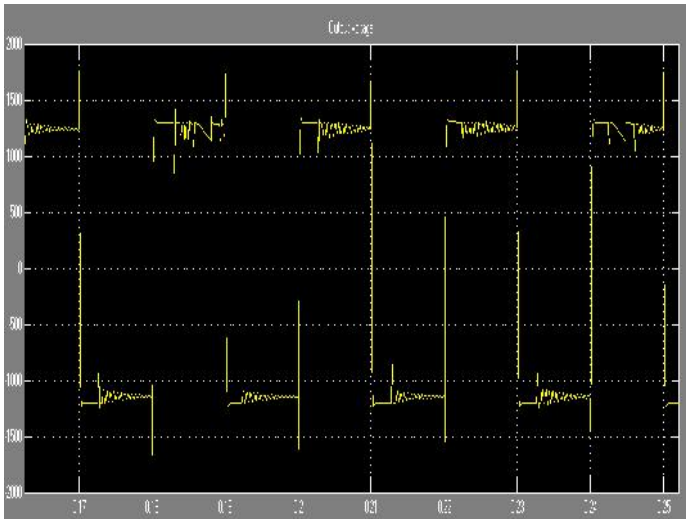

Fig: output voltage

CONCLUSION

A new single-stage multi-input boost converter which can work in both dc–dc and dc–ac modes has been introduced in this paper. The proposed converter is extendable to accept more number of input dc sources, which utilizes minimum number of power switches and small passive elements and does not need any output filter. In the central part of the converter structure battery storage is autonomously charged or discharged to balance the power flow. Two output voltages and several input dc currents control loops have been designed for the proposed converter via integral state feedback control method. The state feedback gain matrixes (*Kx* and *Kq*) are so determined that the converter closed-loop eigenvalues are placed far from *jω*-axis, make the system highly stable and achieve desired dynamic behavior and acceptable transient response. Simulation results show all the converter capabilities such as low-current ripples for input dc sources, autonomous battery charging/discharging, and producing high-quality dc or ac output voltages. A prototype has been also built, which its experimental results verify theoretical and simulation studies.

REFERENCES

[1] Y. Ch. Liu and Y. M. Chen, “A systematic approach to synthesizing multiinput
DC–DC converters,” *IEEE Trans. Power Electron.*, vol. 24, no. 1,pp. 116–127, Jan. 2009.
[2] Y. M. Chen, Y. C. Liu, S. C. Hung, and C. S. Cheng, “Multi-input inverter for grid-connected hybrid PV/Wind power system,” *IEEE Trans. Power Electron.*, vol. 22, no. 3, pp. 1070–1077, May 2007.
[3] L. Yan, R. Xinbo, Y. Dongsheng, L. Fuxin, and C. K. Tse, “Synthesis of multiple-input DC/DC converters,” *IEEE Trans. Power Electron.*, vol. 25, no. 9, pp. 2372–2385, Sep. 2010.
[4] A. Kwasinski, “Identification of feasible topologies for multiple-input DC–DC converters,” *IEEE Trans. Power Electron.*,vol. 24, no. 3, pp. 856– 861, Mar. 2010.
[5] L. Solero, A. Lidozzi, and J. A. Pomilio, “Design of multiple-input power converter for hybrid vehicles,” *IEEE Trans. Power Electron.*, vol. 20, no. 5,pp. 1007–1016, Sep. 2005.
[6] A. Khaligh, J. Cao, and Y. J. Lee, “A multiple-input DC–DC converter topology,” *IEEE Trans. Power Electron.*, vol. 24, no. 3, pp. 862–868, Mar.2009.
[7] F. Nejabatkhah, S. Danyali, S. H. Hosseini, M. Sabahi, and S. A. KH. Mozafari Niapour, “Modeling and control of a new three-input DC–DC boost converter for hybrid PV/FC/battery power system,” *IEEE Trans. Power Electron.*, vol. 27, no. 5, pp. 2309–2324, May 2012.
[8] H. Tao, A. Kotsopoulos, J. L. Duarte, and M. A. M. Hendrix, “Family of multiport bidirectional DC–DC converters,” in *Proc. IEE Elect. Power Appl.*, Apr. 2006, pp. 451–458.
[9] Zh. Qian, O. A. Rahman, H. A. Atrash, and I. Batarseh, “Modeling and control of three-port DC/DC converter interface for satellite applications,” *IEEE Trans. Power Electron.*, vol. 25, no. 3, pp. 637–649, Mar. 2010.
[10] Zh.Qian,O. A. Rahman, and I. Batarseh, “An integrated four-port DC/DC converter for renewable energy applications,” *IEEE Trans. Power Electron.*, vol. 25, no. 7, pp. 1877–1887, Jul. 2010.
[11] H.Wu, K. Sun, S. Ding, and Y. Xing, “Topology derivation of non isolated three-port DC–DC converters from DIC and DOC,” *IEEE Trans. Power Electron.*, vol. 28, no. 7, pp. 3297–3307, Jul. 2013.
[12] Y-M Chen, A. Q. Huang, and X. Yu, “A high step-up three-port DC-DC converter for stand-alone PV/battery power systems,” *IEEE Trans. Power Electron.*, to be published.
[13] M. Sarhangzadeh, S. H. Hosseini, M. B. B. Sharifian, and G. B. Gharehpetian, “Multi-input direct DC-AC converter with high frequency link for clean power generation systems,” *IEEE Trans. Power Electron.*, vol. 26, no. 6, pp. 625–631, Jun. 2011.
[14] J. L. Duarte, M. Hendrix, and M. G. Simoes, “Three-port bidirectional converter for hybrid fuel cell systems,” *IEEE Trans. Power Electron.*, vol. 22, no. 2, pp. 480–487, Mar. 2007.
[15] H. Tao, J. L. Duarte, and M. A. M. Hendrix, “Line-interactive UPS using a fuel cell as the primary source,” *IEEE Trans. Ind. Electron.*, vol. 51,no. 3, pp. 3012–3021, Aug. 2008.
[16] Y. M. Chen, Y. Ch. Liu, Sh. Ch. Hung, and Ch. Sh. Cheng, “Multi-input inverter for grid-connected hybrid PV/Wind power system,” *IEEE Trans. Power Electron.*, vol. 22, no. 3, pp. 1070–1077, May 2007.
[17] Y. Zhou and W. Huang, “Single-stage boost inverter with coupled inductor,” *IEEE Trans. Power Electron*, vol. 27, no. 4, pp. 1885–1893, Apr.2012
[18] F. Z. Peng, M. Shen, and K. Holland, “Application of Z-source inverter for traction drive of fuel cell-battery hybrid electric vehicles,” *IEEE Trans. Power Electron.*, vol. 22, no. 3, pp. 1054–1061, May 2007.